

## Chapter 2 Theory

### 2.1 Global Minimization of the Pressure Field in a 3-D Cavity

A study of the references on active control applied to automobile cabin noise show evidence that the most useful criterion to achieve global control in an enclosure turns out to be the minimization of the total acoustic potential energy [3]. This minimization strategy may increase the level at positions where the level was originally low, but it has the effect of leveling the spatial variation of pressure since dominant acoustic modes are suppressed.

The discussion presented in this chapter covers the theory required to simulate Active Noise Control in a cavity. The expressions derived are valid for any number of actuators and sensors. The approach is essentially that suggested by Piraux and Nayrolles [39], and is somewhat analogous to that used by Burdess and Metcalfe [40] in that it minimizes the total time average strain energy in a vibrating system.

The total acoustic potential energy  $E$  in a cavity can be expressed as:

$$E = \frac{1}{4\rho c^2} \int_V |p|^2 dV, \quad (2.1)$$

where  $c$  is the speed of sound in air ( $340 \text{ m}\cdot\text{s}^{-1}$ ),  $\rho$  is the density of air ( $1.21 \text{ kg}\cdot\text{m}^{-3}$ ),  $V$  is the volume of the cavity, and  $p$  the pressure at any point in the cavity.

The pressure at the  $i^{\text{th}}$  sensor ( $P_i$ ) is due to both the disturbance ( $P_{\text{idist}}$ ) and each secondary source ( $P_{\text{iactl}}$ ). Since linearity is assumed through the entire discussion, this can be expressed as:

$$P_i(\omega) = P_{\text{idist}}(\omega) + \sum_{l=1}^{\text{Nba}} P_{\text{iactl}}(\omega). \quad (2.2)$$

Let  $B_{il}(\omega)$  be the transfer function between the strength of actuator  $l$  ( $Q_l(\omega)$ ) and the pressure sensed by the  $i^{\text{th}}$  sensor. Using the transfer function and substituting into equation (2.2), a relationship between the strength of each actuator and pressure at sensor  $i$  is found:

$$P_i(\omega) = P_{\text{idist}}(\omega) + \sum_{l=1}^{\text{Nba}} B_{il}(\omega) * Q_l(\omega). \quad (2.3)$$

Substituting the expression found for  $P_i(\omega)$  in a discretized form of equation (2.1), an expression for the cost function  $E$  is obtained. This expression will be minimized in terms of the strength of each actuator and for each frequency  $\omega$ :

$$E = cst * \sum_{i=1}^{\text{Nbs}} \left[ P_{\text{idist}}(\omega) + \sum_{l=1}^{\text{Nba}} B_{il}(\omega) * Q_l(\omega) \right]^2. \quad (2.4)$$

Equation (2.4) can be expressed in matrix form:

$$E = (\mathbf{P} + \mathbf{B}\mathbf{X})^H (\mathbf{P} + \mathbf{B}\mathbf{X}), \quad (2.5)$$

where  $\mathbf{X}$ , the source strength, is the unknown. Assuming a fully determined system (i.e., the number of actuators and sensors is the same), it can be shown that for an optimized  $\mathbf{X}$ ,  $E = 0$ .

The experiments presented in section 4.3 and performed using feedforward control showed that in a practical case the cost function  $E$  can not be driven to zero even in the case of a fully determined system. For this reason, another cost function ( $J$ ) is defined. An offset pressure ( $P_{\text{off}}$ ) is defined for each error sensor such that the algorithm converges to the sum of the offset pressure squared.  $J$  is expressed as follows:

$$J = (\mathbf{P} + \mathbf{P}_{\text{off}} + \mathbf{B}\mathbf{X})^H (\mathbf{P} + \mathbf{P}_{\text{off}} + \mathbf{B}\mathbf{X}). \quad (2.6)$$

Optimization of  $J$  leads to:

$$\mathbf{X}_{\text{opt}} = -(\mathbf{B}^H \mathbf{B})^{-1} \mathbf{B}^H (\mathbf{P}_{\text{off}} + \mathbf{P}). \quad (2.7)$$

Expressing J in terms of E gives:

$$J = E + \mathbf{P}_{off}^H \mathbf{P}_{off} + \mathbf{P}_{off}^H \mathbf{P} + \mathbf{P}^H \mathbf{P}_{off} + \mathbf{P}_{off}^H \mathbf{B} \mathbf{X} + \mathbf{X}^H \mathbf{B}^H \mathbf{P}_{off} \quad (2.8)$$

Knowing that  $\mathbf{B} \mathbf{X}_{opt} = -(\mathbf{P}_{off} + \mathbf{P})$ , the expression of J after optimization can be expressed by:

$$J_{opt} = E_{opt} + \mathbf{P}_{off}^H \mathbf{P}_{off} \quad (2.9)$$

In the case where the system is fully determined (i.e., the number of actuators is the same as the number of error sensors),  $J_{opt} = \mathbf{P}_{off}^H \mathbf{P}_{off}$ .

In order to validate this model, simulations have been performed in a rectangular cavity (see Figure 2.1). The configuration of the actuators and the error sensors was different in each simulation. The optimized cost function was computed for frequencies below 200 Hz and results are presented in Figures 2.2 and 2.3 for two of the configurations.

The cavity has the following characteristics:

- The volume is 1.5 by 1.5 by 3m, meshed with linear bricks, which have 1 node per vertex. Four elements have been used on the 1.5m length, and six elements have been used on the 3m length. Increasing the number of elements did not improve the accuracy of the results at frequencies below 200 Hz. Thus, no more elements were used in order to reduce the computation time.
- The acoustic medium is defined as air ( $c=340\text{m}\cdot\text{s}^{-1}$ ,  $\rho=1.2\text{ kg}\cdot\text{m}^{-3}$ )
- The disturbance is the vibration of the plane defined by  $z=3$  (velocity boundary condition:  $0.01\text{ ms}^{-1}$  in magnitude and no phase).
- The Finite Element analysis was limited to frequencies below 200 Hz and was performed using the commercial code Sysnoise [41]. All the walls are defined as rigid and fixed, with the exception of the disturbance plate. This analysis provides the transfer functions  $B_{il}(\omega)$  and  $P_{idist}(\omega)$ , used to form the matrices B and P used in equation (2.7).
- Implementation of equation (2.7) was performed using Matlab [42].

In the first configuration, one actuator and six error sensors are used. The actuator is a spherical source located in the center of the wall opposite to the disturbance. The sensors are

evenly spaced along the axis perpendicular to the disturbance, as illustrated in Figure 2.1. Figure 2.2 shows the total acoustic potential energy before and after control. The energy has been computed using all the nodes of the mesh (175 nodes). The control achieved with this configuration is excellent, since all the resonant peaks are cancelled. As illustrated in Figure 2.2, the frequency response is flat in the frequency band of interest. These results are very similar to those obtained by Nelson, et al [3]. It can be concluded therefore that the model described in this section provides accurate results for the simulation of active noise control in an enclosure.

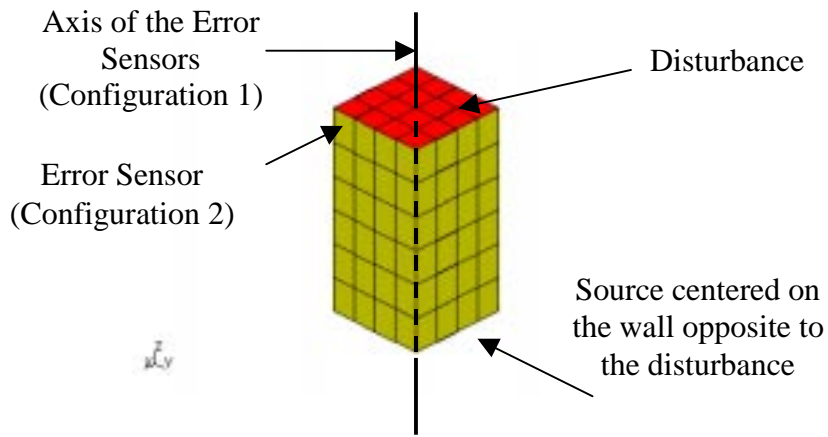


**Figure 2.1** Finite element model of the cavity with the control source and the error sensors

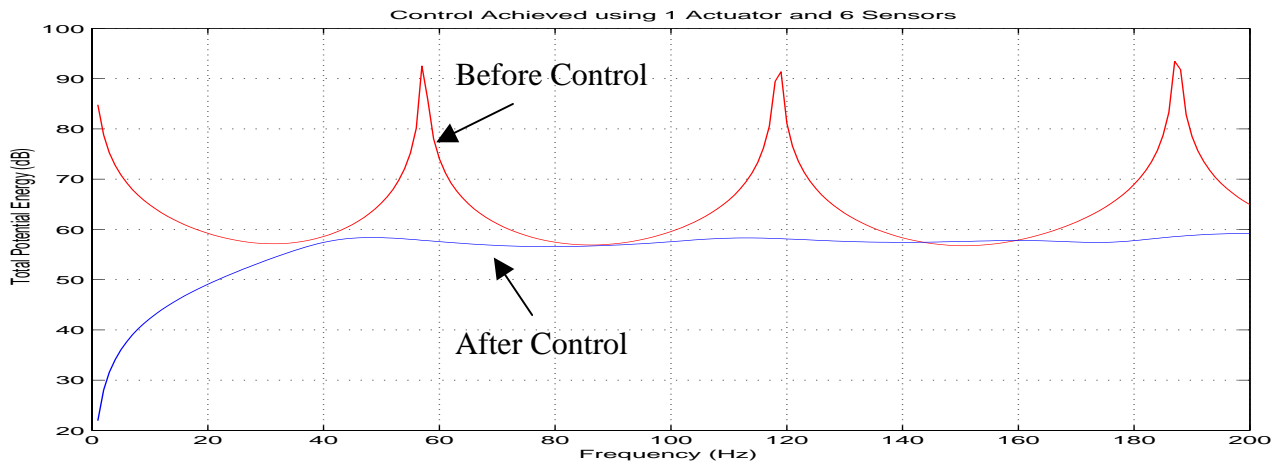


**Figure 2.2** Control using 1 actuator and 6 sensors in a rigid rectangular box

A simulation was performed to illustrate the spatial spillover, which occurs when the minimization of the cost function at arbitrary error signal locations leads to an increase of the pressure level at other locations. In this simulation, the actuator is located at the center of the wall opposite the disturbance (this is the same location as in the previous configuration), and one error sensor is located in one corner of the rectangular cavity. The result is illustrated in Figure 2.3.

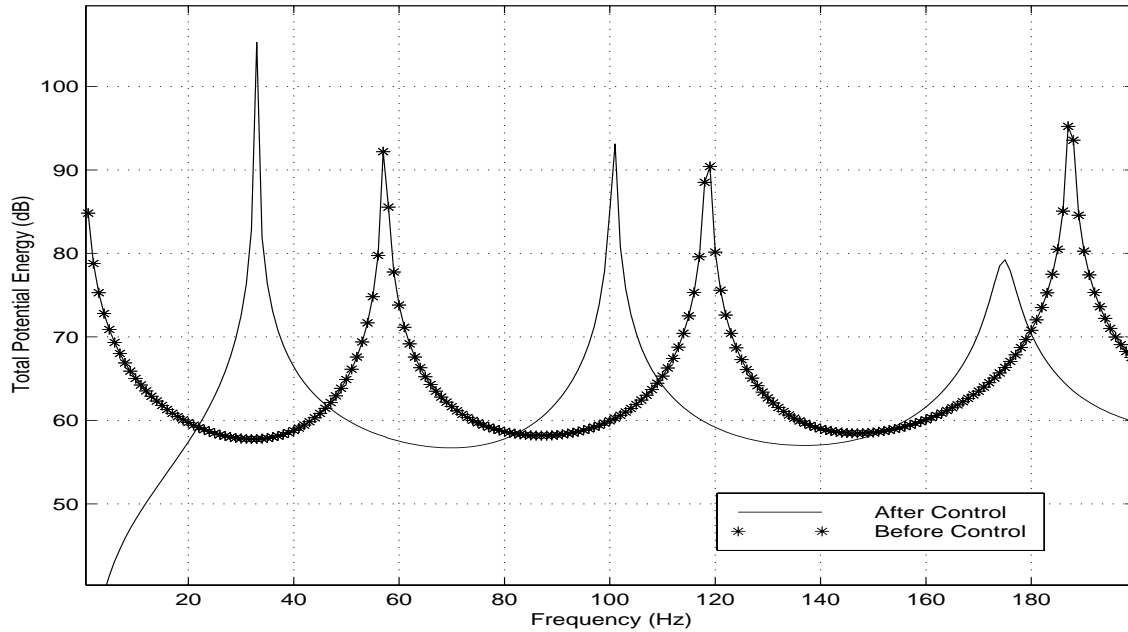


**Figure 2.3** Control involving improper sensor locations

According to Figure 2.3, a peak appears around 30 Hz after control. Since the modal analysis of the box shows that the first resonant frequency is at 57 Hz, the peak is not due to the excitation of a new mode.

The transfer function between the actuator and the error signal is shown in Figure 2.4.(a). The transfer functions between the actuator and three sensors used to compute the total acoustic potential energy in the box are shown in Figure 2.4 (b). Figure 2.4 (a) also shows an anti-resonance at the frequency where the first peak appears after control. This anti-resonance means that a high input is required to raise the pressure level at the sensor location in order to achieve some control. Figure 2.4 (a) also shows a phase shift of 180 degrees at 30 Hz, which means a poor control authority at that frequency. On the other hand, there is no anti-resonance at this same frequency on the transfer functions of the sensors used to compute the energy, therefore, no

phase shift. Hence, the interference is constructive instead of destructive, and the high input leads to a high output, which results in a large increase of the pressure level at this location. This effect is apparent in Figure 2.3.

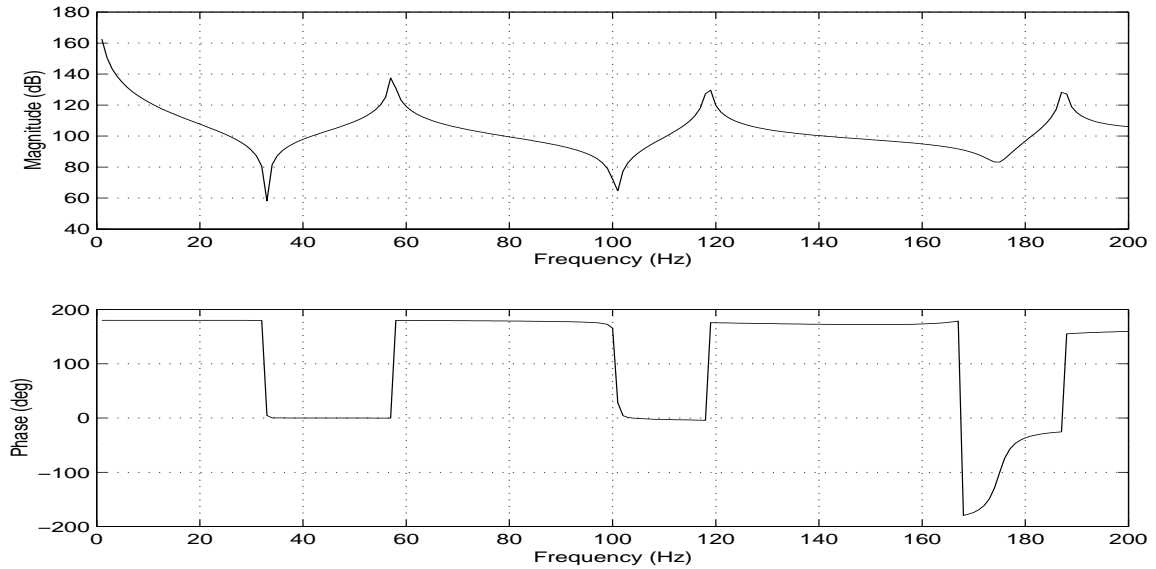


**Figure 2.4 (a)** Transfer functions between actuator and error sensor

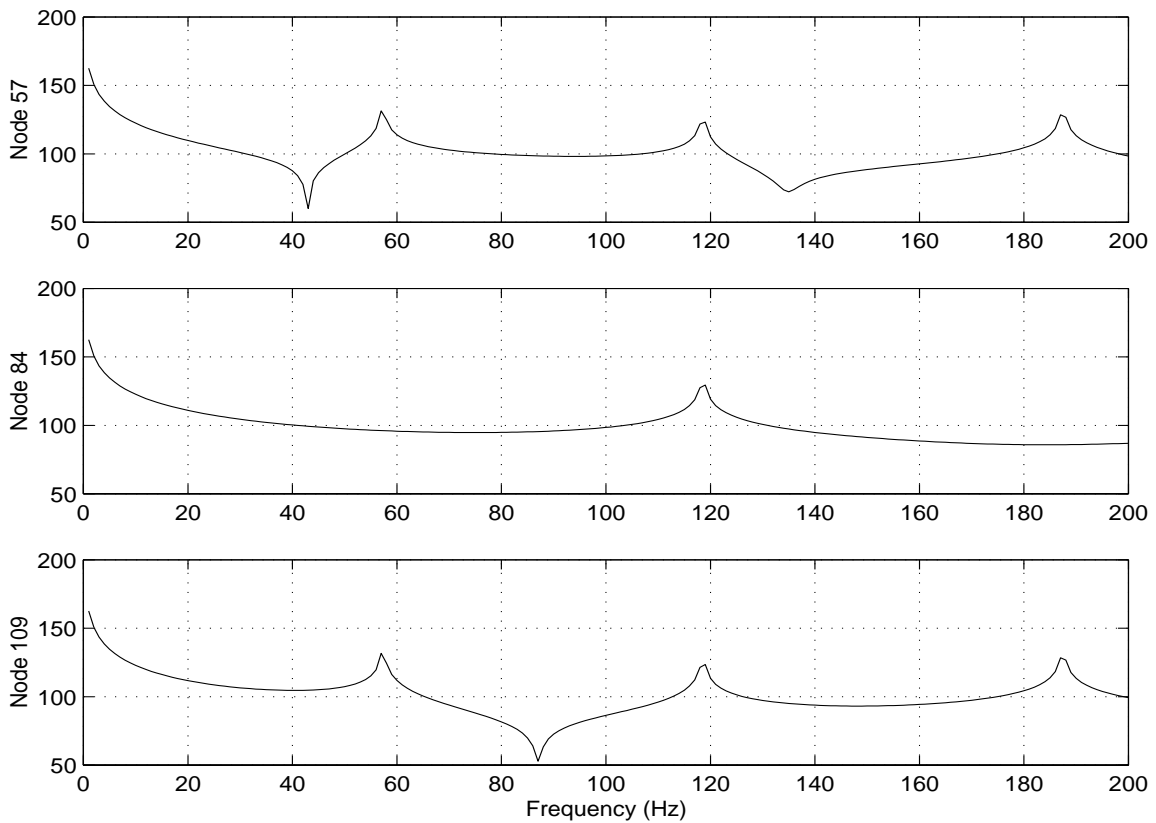


**Figure 2.4 (b)** Transfer functions between actuator and sensors.

## 2.2 Genetic Algorithms for Optimization

An important consideration in the design of an Active Noise Control system for interior problems is the location of the actuators and sensors. A first approach consists of choosing positions that couple well with the modes excited by the disturbance in the frequency band of interest (i.e., at the antinodes of the mode) [4]. As the frequency band becomes fairly wide and the frequencies of interest high, the number of modes, which contributes to the acoustic response, increases quickly. The problem is such that, with a finite set of actuators and sensors, the localization of the transducers is not straightforward and becomes a trade off among the degrees of freedom of the system (modes).

Optimization techniques used in engineering can be divided into three different types: enumerative, calculus based, and random search [43]. Enumerative searches compare cost function values at each point of a discrete space. Such techniques are very good in finding the true optimum of a function, but are generally not applicable to problems with high dimensionality. Calculus based optimizations search for a zero gradient either directly or by means of a gradient search method. This technique is effective for analytical work but is ill suited for experimental applications, especially those involving discontinuities, where the gradient is not defined. The last class of optimization methods includes simple random walks and directed searches with randomized or probabilistic decision making. An example of this last type is the genetic algorithm (GA). Nowadays the GA technique is very popular in experimental work since it requires low computation time to locate the optimum of a function.

GAs [43], first developed by Holland [44], are an important branch of the more general field of evolutionary algorithms [45, 46]. GAs use idealized operators to mimic the process of Darwinian natural selection on a population of candidate solutions. In GAs, the population is made of a fixed-length string, which is a representation of the problem. Each string is a potential solution, and the set of strings goes through all the Darwinian reproduction operators.

A schematic of a simple GA implementation is shown in Figure 2.5. In the preliminary step of the algorithm, the initial population is computed. This operation may be either done randomly or predefined by the user. In a second step, four selection operations are performed successively in a loop until the convergence criteria is met.

First, a fitness value is computed for each member of the generation according to the analytical objective value or cost function. Second, the reproduction operator for inclusion in the next generation selects the members with a probability proportional to their fitness value. Third, the crossover operator simulates a mating process by randomly exchanging genetic information between a pair of members. This exchange is performed with probability  $P_c$  by partial string exchanges. Fourth, the mutation operator exchanges a random element of the string with probability  $P_m$ . This operator adds robustness to the process by preventing the algorithm to concentrate on a small area of the search space.

Some important issues must be addressed at this point. First, GAs operate on a coding of the problem's parameter set, not the parameters themselves, and different coding schemes may result in different algorithm behavior. GAs must be tuned to an individual problem to ensure the best performances since the different steps of the algorithm are specific (i.e., it is the user's responsibility to choose the population size and the probabilities for crossover and mutation,  $P_c$  and  $P_m$  respectively).

GAs have recently been used for position optimization of actuators and sensors in various applications [47-49]. In the research work presented here, the algorithm is applied to the location of the actuators and sensors in a three dimensional cavity for global active noise control using a filtered-X feedforward approach.



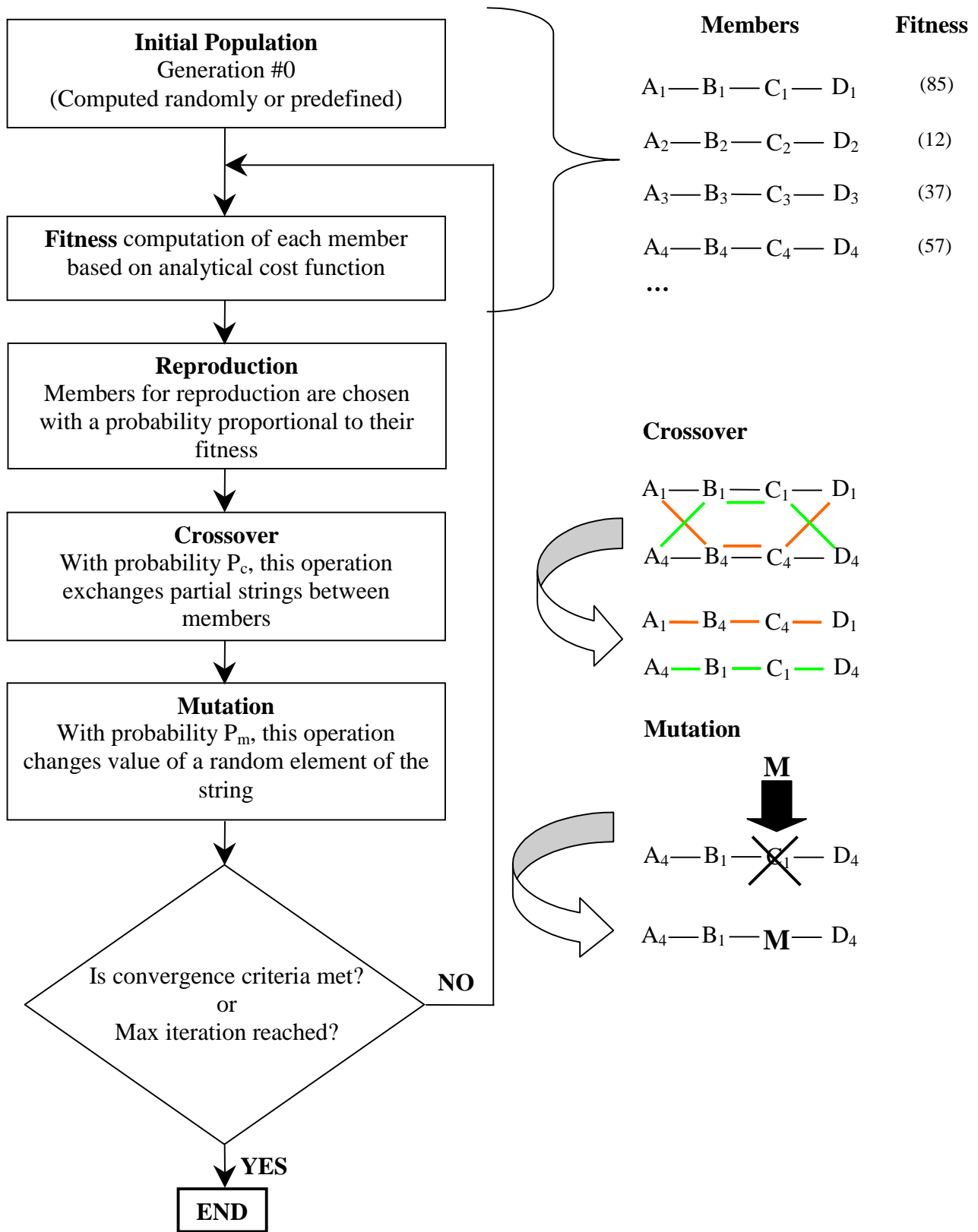


**Figure 2.5** Schematic of simple genetic algorithm

## 2.3 The Feedforward Filtered-X LMS Algorithm

The control approach used to perform the Active Noise Control procedure is the filtered-X algorithm, an alternative form of the standard LMS algorithm [50]. The filtered-X LMS algorithm was first developed by Widrow and Burgess [50]. The discussion below describes each step necessary to implement the algorithm presented in Figure 2.6. Derivation of the equations used in this algorithm is also included in the discussion. The equations provided assume a single input single output system (SISO).

In the standard LMS algorithm an L-delay-element vector  $\mathbf{W}(k)$  is computed to filter the reference vector  $\mathbf{X}(k)$ . The resulting vector  $\mathbf{Y}(k)$  is the output signal to the actuator.

$$\mathbf{Y}(k) = \mathbf{W}(k)^T \mathbf{X}(k), \quad (2.10)$$

where  $\mathbf{W}(k) = [a_0(k) a_1(k) \dots a_L(k)]$  and  $\mathbf{X}(k) = [x(k) x(k-1) \dots x(k-L)]^T$ .

$\mathbf{X}(k)$  is also known as the reference signal and must be well correlated with the signal being cancelled. The maximum achievable reduction depends on the coherence function between the reference and error signals (discussed in chapter 5.1).

The algorithm uses either finite impulse response filters (FIR) or infinite impulse response filters (IIR) to form  $\mathbf{W}(k)$ . The vector  $\mathbf{W}(k)$  is iteratively modified by an amount proportional to the gradient of the square of the instantaneous error  $e(k)$  between the actual plant output and the modeled output. This process is given by equation (2.11):

$$\mathbf{W}(k+1) = \mathbf{W}(k) + \mu \frac{\partial E[e^2(k)]}{\partial \mathbf{W}(k)}, \quad (2.11)$$

where  $\mu$  is the convergence factor. It is important to note that if  $\mu$  is too high, the algorithm may diverge. The maximum value is defined by Widrow, et al [50] as:

$$\mu_{\max} \leq \frac{1}{L \cdot P(x)} \quad (2.12)$$

Since the desired output  $d_k$  does not depend on  $\mathbf{W}(k)$ , the gradient of the square of the error signal is simply twice the product of the error by the gradient of the reference signal. It can also be shown that the gradient of the model output with respect to the weight vector  $\mathbf{W}(k)$  is simply the input vector  $\mathbf{X}(k)$  [50]. Therefore, the equation for weight update can be expressed as:

$$\mathbf{W}(k+1) = \mathbf{W}(k) + 2\mu e(k)\mathbf{X}(k). \quad (2.13)$$

In the case of the filtered-X algorithm, the reference signal  $\mathbf{X}(k)$  is filtered prior to the weight update procedure of the LMS algorithm. This technique provides a signal that is insensitive to plant disturbances, ensures rapid convergence, and tracks the disturbance signal. The filter ( $\mathbf{T}_{ce}^*$ ) is a FIR or IIR filter, which is a model of the transfer function  $T_{ce}$  between the actuators and error sensors. Finally, the weight update equation takes the form given by:

$$\mathbf{W}(k+1) = \mathbf{W}(k) + 2\mu e(k)\mathbf{T}_{ce}^* \mathbf{X}(k) \quad (2.14)$$

The filter  $\mathbf{T}_{ce}^*$  is determined off-line prior to the control during the system identification. In this procedure, each actuator at a time is driven with white noise and the LMS algorithm is used to identify each path of the plant.

The use of multiple error microphones, an extension to this discussion, has been presented by Elliott et al [51]. Practical application using multiple actuators, error microphones, and reference signals has been shown by Sutton, et al [29]. As discussed by Fuller [4], if all the error signals are equally weighted, and no effort term is used, the update equation for each control filter coefficient becomes:

$$W_{mki}(n+1) = W_{mki}(n) - \mu \sum_{l=1}^L r_{lmk}(n)e(n-i) \quad (2.15)$$

where  $r_{lmk}$  is the filtered reference signal obtained by passing the reference sensor signal  $x_k(n)$  through an estimate of the path from the  $m$ -th actuator to the  $l$ -th error sensor,  $G_{lm}(q)$ .

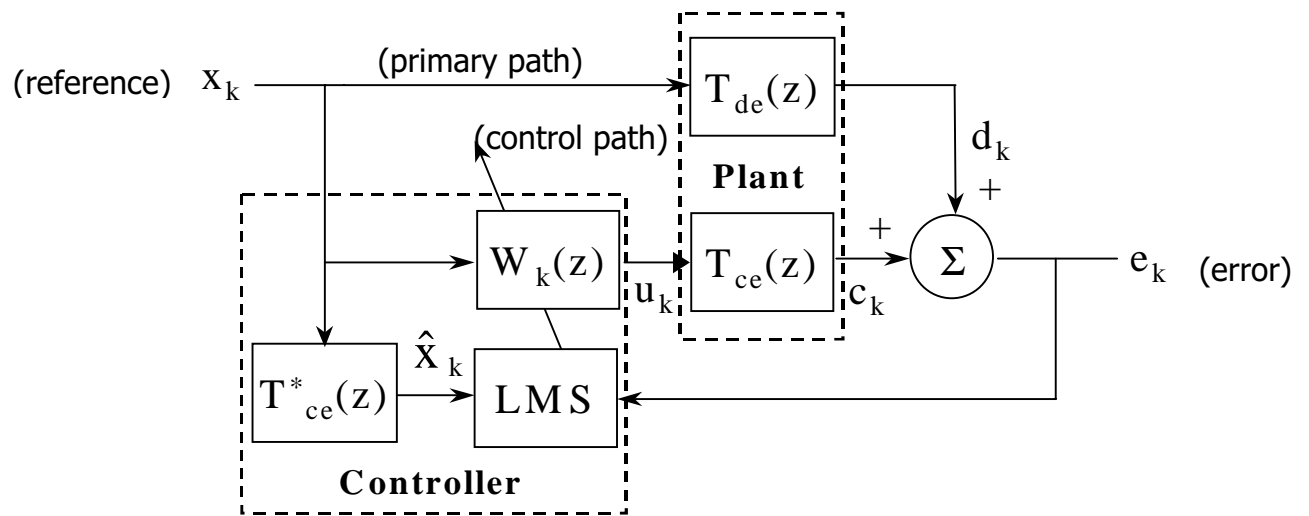


**Figure 2.6** Block diagram of the Filtered-X LMS Algorithm